



Original Article



A Prognostic Nomogram with High Accuracy Based on 2D-SWE in Patients with Acute-on-chronic Liver Failure

Lili Wu^{1#}, Jieyang Jin^{1#}, Taicheng Zhou², Yuankai Wu³, Xinhua Li³, Xiangyong Li³, Jie Zeng¹, Jinfen Wang¹, Jie Ren^{1*}, Yutian Chong³ and Rongqin Zheng¹

¹Department of Medical Ultrasonics, Third Affiliated Hospital of Sun Yat-Sen University, Guangdong Key Laboratory of Liver Disease Research, Guangzhou, Guangdong, China; ²Department of Gastroenterological Surgery and Hernia Center, Sixth Affiliated Hospital of Sun Yat-Sen University, Guangdong Institute of Gastroenterology, Guangdong Provincial Key Laboratory of Colorectal and Pelvic Floor Diseases, Supported by National Key Clinical Discipline, Guangzhou, Guangdong, China; ³Department of Infectious Diseases, Third Affiliated Hospital of Sun Yat-Sen University, Guangzhou, Guangdong, China

Received: 12 July 2021 | Revised: 22 November 2021 | Accepted: 29 November 2021 | Published: 13 January 2022

Abstract

Background and Aims: Acute-on-chronic liver failure (ACLF) is associated with very high mortality. Accurate prediction of prognosis is critical in navigating optimal treatment decisions to improve patient survival. This study was aimed to develop a new nomogram integrating two-dimensional shear wave elastography (2D-SWE) values with other independent prognostic factors to improve the precision of predicting ACLF patient outcomes. **Methods:** A total of 449 consecutive patients with ACLF were recruited and randomly allocated to a training cohort ($n=315$) or a test cohort ($n=134$). 2D-SWE values, conventional ultrasound features, laboratory tests, and other clinical characteristics were included in univariate and multivariate analysis. Factors with prognostic value were then used to construct a novel prognostic nomogram. Receiver operating curves (ROCs) were generated to evaluate and compare the performance of the novel and published models including the Model for End-Stage Liver Disease (MELD), MELD combined with sodium (MELD-Na), and Jin's model. The model was validated in a prospective cohort ($n=102$). **Results:** A ACLF prognostic nomogram was developed with independent prognostic factors, including 2D-SWE, age, total bilirubin (TB), neutrophils (Neu), and the international normalized ratio (INR). The area under the ROC curve (AUC) was 0.849 for the new model in the training cohort and 0.861 in the prospective validation cohort, which were significantly greater than those for MELD (0.758), MELD-Na (0.750), and Jin's model (0.777, all $p < 0.05$). Calibration curve analysis revealed

good agreement between the predicted and observed probabilities. The new nomogram had superior overall net benefit and clinical utility. **Conclusions:** We established and validated a 2D-SWE-based noninvasive nomogram to predict the prognosis of ACLF patients that was more accurate than other prognostic models.

Citation of this article: Wu L, Jin J, Zhou T, Wu Y, Li X, Li X, et al. A Prognostic Nomogram with High Accuracy Based on 2D-SWE in Patients with Acute-on-chronic Liver Failure. J Clin Transl Hepatol 2022;10(5):803–813. doi: 10.14218/JCTH.2021.00278.

Introduction

Acute-on-chronic liver failure (ACLF) is a serious clinical condition associated with high short-term mortality.^{1–3} It has been estimated that approximately 50% of ACLF patients have no identifiable triggers.¹ In China, hepatitis B virus (HBV) infection has been recognized as the most common etiology for ACLF, which is mainly attributable to a relatively high incidence of HBV infection in the country.^{3,4} Patients with ACLF caused by HBV infection or acute-on-chronic hepatitis B liver failure (ACLF-HBV) are characterized by the sudden onset and rapid progression of ACLF and high risk of short-term death, which the treatment off ACLF-HBV challenging.^{5,6} Currently, liver transplantation (LT) is the only curative treatment of ACLF and ACLF-HBV patients who have failed medical treatment.^{6,7} Obviously, early and accurate prediction of prognosis is critical in navigating optimal treatment decisions that lead to improved survival.⁸

The Model for End-Stage Liver Disease (MELD) score, a well-validated standard scoring system, is used to prioritize organ allocation to patients diagnosed with end-stage liver disease in need of LT and as a prognostic tool for ACLF.⁹ In addition to MELD, a number of prognostic scoring systems and models, including our proposed nomogram, have been developed to predict the prognosis of ACLF patients. However, the existing prognostic models are not satisfactory and, lack predictive accuracy.

Advances in ultrasonography such as transient elastography (TE) and two-dimensional shear-wave elastography

Keywords: Acute-on-chronic liver failure; Two-dimensional shear wave elastography; Hepatitis B virus; Prognosis.

Abbreviations: ACLF, acute-on-chronic liver failure; ACLF-HBV, acute-on-chronic hepatitis B liver failure; AUC, area under the curve; CI, confidence interval; 2D-SWE, two-dimensional shear wave elastography; HBV, hepatitis B virus; LSM, liver stiffness measurement; LT, liver transplantation; MELD, Model for End-stage Liver Disease; MELD-Na, Model for End-stage Liver Disease score combined with sodium; ROC, receiver operating characteristic; TB, total bilirubin; TE, transient elastography.

[#]Both authors contributed equally to this work.

*Correspondence to: Jie Ren, Department of Medical Ultrasonics, Third Affiliated Hospital of Sun Yat-Sen University, 600 Tianhe Road, Guangzhou, Guangdong 510630, China. ORCID: <https://orcid.org/0000-0003-2599-9001>. Tel: +86-20-85252010, Fax: +86-20-87583501, E-mail: renj@mail.sysu.edu.cn

(2D-SWE) allow noninvasive liver stiffness measurement (LSM).^{10–16} We recently evaluated the accuracy of 2D-SWE to predict the prognosis of patients with ACLF-HBV. Our data, together with those of previous studies demonstrated that 2D-SWE was better and more suitable than TE for LSM of patients with ACLF.^{17–24} Subsequently, we established a prognostic model (Jin's model) based on 2D-SWE values in combination with MELD for the prediction of the prognosis of patients with ACLF-HBV.²⁰ Jin's model (previously the MELD-SWE score) was shown superior to MELD alone in predicting the prognosis of ACLF-HBV patients.²⁰ However, until now, a prognostic model combining 2D-SWE with other independent prognostic factors obtained prospectively from ACLF-HBV patients has not been reported. Intrigued by the prognostic value of 2D-SWE and based on our previous findings, this prospective study was aimed to develop and validate a novel nomogram by integrating 2D-SWE values with other independent prognostic factors. The findings of this study are expected to provide a better model for predicting the prognosis of patients with ACLF.

Methods

Patient enrollment

Patients were consecutively screened for their eligibility to participate in this study at the Third Affiliated Hospital of Sun Yat-Sen University (Guangzhou, Guangdong, China) between November 2013 and August 2016. The patient enrollment process is shown in Supplementary Figure 1. The inclusion criteria were: (1) ACLF caused by HBV infection; (2) the diagnosis of ACLF was made following the criteria the Asian Pacific Association for the Study of the Liver.⁸ The exclusion criteria were: (1) ACLF with causes other than HBV infection, such as hepatitis C virus (HCV) infection, alcoholic liver disease, drug-induced hepatitis, autoimmune liver disease, or Wilson's disease; and (2) lost to follow-up. A total of 449 patients with ACLF caused by HBV infection were recruited and were randomly allocated in a 2:1 ratio to a training cohort ($n=315$) and a test cohort ($n=134$). A group of 102 ACLF patients were prospectively enrolled in a validation cohort at the Third Affiliated Hospital of Sun Yat-Sen University between September 2019 and October 2021.

Prior to enrollment, written informed consent was obtained from each patient. The study was reviewed and approved by the Human Research Ethic Committee of the Third Affiliated Hospital of Sun Yat-Sen University [no. (2020) 02-253-01]. The study protocol conformed to the ethical guidelines of the 1975 Declaration of Helsinki.

Treatment, follow-up, and prognosis

The enrolled patients received standard treatment as previously described,³ follow-up for at least 90 days, or until death or liver transplantation, starting at the time of diagnosis with ACLF. The prognosis of each patient was categorized as either a survivor, with 3 months of liver transplant-free survival or a nonsurvivor. Survival was defined as the resolution of ACLF and cessation of intensive treatment such as artificial liver support. Nonsurvival was defined as patient death or need of liver transplantation because of lack of response to intensive treatment within the 90 days of follow-up.

Measurement of liver stiffness with 2D-SWE

2D-SWE was performed on each patient after hospital ad-

mission as previously reported.²⁰ In brief, liver stiffness was measured by ultrasonography (US) using an Aixplorer system (SuperSonic Imagine, Aix-en-Provence, France) with an SC6-1 convex probe (1–6 MHz). A 4 cm × 3 cm 2D-SWE rectangular elasticity box was placed 1–2 cm under the liver capsule in a parenchyma area free of large vessels. Two examiners with experience in performing over 500 2D-SWEs, performed the procedures and were blinded to the patients' clinical and laboratory data. The median of five independent kPa values was used in the analysis.

Conventional US

Conventional B-mode US was performed after completion of 2D-SWE. Ten parameters were measured: liver surface, liver parenchyma, thickness of the right lobe, biliary sludge, thickness of the gallbladder wall, presence of gallbladder enlargement, spleen index (length, thickness), ascites index (maximum depth of ascites), diameter of the portal vein, and re-opening of the paraumbilical vein, as previously reported.^{20,25} Gallbladder enlargement was defined as a length >90 mm and/or an anterior-posterior diameter >40 mm. Biliary sludge was defined as presence of low-level echoes without posterior acoustic shadowing and a shift with position changes. The ascites index was calculated as the maximum depth of ascites. The spleen index was recorded as the product of the longitudinal and transverse diameters of the spleen.

Laboratory tests

Blood samples were collected from the patients, and laboratory testing was performed to determine alanine aminotransferase, aspartate aminotransferase, gamma-glutamyl transpeptidase, and alkaline phosphatase levels; total bilirubin, albumin, total cholesterol, serum creatinine, serum sodium, prothrombin time, prothrombin activity, international normalized ratio, white blood cell count, platelet count, and hemoglobin. Patients were also tested for markers of HBV infection, including hepatitis B e antigen, hepatitis B surface antigen, and HBV DNA viral load.

Development of a new nomogram to predict prognosis in the training cohort

2D-SWE values, conventional B-mode US, laboratory test results, and demographic and clinicopathological characteristics of the ACLF patients in the training cohort were included in univariate regression analysis to identify factors significantly associated with prognosis. Multivariate regression analysis of factors with potential prognostic value was then used in to identify independent prognostic factors. Events included in the multivariate analysis included deaths from ACLF, and underwent LT within 3 months of ACLF. Patients who survived longer than 3 months were recorded as nonevents. 2D-SWE values and the factors independently associated with the prognosis were then employed to construct the novel prognostic nomogram.

Performance evaluation and validation of the nomogram for predicting prognosis

The performance of the new model was evaluated and compared with existing prognostic prediction scoring models, including MELD, MELD combined with sodium (MELD-Na), and the previously reported Jin's model.²⁰ The MELD score

$R = 3.8 \ln [\text{bilirubin (mg/dL)}] + 11.2 \ln (\text{INR}) + 9.6 \ln [\text{creatinine (mg/dL)}] + 6.4 (\text{cause of cirrhosis: cholestatic or alcoholic 0, other 1})$. The MELD-Na score = $\text{MELD} + 1.59 \times [135 - \text{Na (mmol/L)}]$, Na = serum sodium >135 mmol/L was calculated as 135, and serum sodium <120 mmol/L was calculated as 120. Jin's model score = $\text{MELD} - \text{SWE} = 1.3 \times \text{MELD} + 0.3 \times 2\text{D-SWE (kPa)}$ (MELD-SWE score).

Decision curves of the models were plotted, and decision-curve analysis (DCA) was performed to evaluate the clinical utility and net benefit. Calibration curves were created to evaluate the agreement between the predicted and observed probability. For assessment of predictive accuracy, receiver operating curves (ROCs) were generated to calculate standard indices.

Statistical analysis

Statistical analysis was performed with IBM SPSS Statistics 25 for Windows (IBM Corp., Armonk, NY, USA), R (version 3.6.2), and MedCalc (version 19.8) statistical software. Continuous data were reported as means±standard deviation or medians and interquartile range, as appropriate. Student's *t*-test or the Mann-Whitney U test was used to compare differences between groups. Categorical data were reported as numbers and percentages (%), and chi-square test or Fisher's exact test was used to compare difference between groups. Survival probability curves were plotted by the Kaplan-Meier method and between-differences were compared using log-rank tests. Univariate and multivariate Cox proportional hazards analyses were performed to evaluate the association of each variable and clinical outcome. ROC curve characteristics and the area under the ROC curve (AUC) were used to evaluate the prediction of prognosis. DeLong's test was used to compare differences of the AUC values of prognostic models. *P*-values <0.05 was considered statistically significant.

Results

Demographic and clinicopathologic characteristics of the patients

During the study period, 449 consecutive patients with ACLF caused by HBV infection were randomly assigned to training (*n*=315) and test (*n*=134) cohorts. Baseline demographic characteristics, clinicopathologic features, and laboratory testing data are summarized in Table 1. The demographic characteristics were similar, and there were no significant differences in age and sex between the training and test cohorts. Conventional US parameters and 2D-SWE values in the training and test cohorts were comparable.

The prognosis of each patient was classified as 'survivor' or 'nonsurvivor' on the basis of the 90-day follow-up, and no significant difference was observed between the training and test cohorts.

Univariate and multivariate analysis of factors associated with the prognosis of ACLF patients in the training cohort

Univariate analysis was performed to identify factors significantly associated with prognosis. As shown in Table 2, variables including age, conventional US parameters (i.e., liver capsule, thickness of right liver lobe, gallbladder wall thickness, and gallstones), 2D-SWE measurements, and some laboratory tests were significantly associated with

patient prognosis in the training cohort. The results of multivariate logistic regression analysis [odds ratios (ORs) with 95% confidence intervals (CIs) are shown in Table 3. The variables independently associated with the prognosis of patients with ACLF caused by HBV infection were age (OR: 1.04, 95% CI 1.01–1.08), TB (OR: 1.01, 95% CI: 1.00–1.01), Neu (OR: 139.55, 95% CI: 6.41– 3,037.71), INR (OR: 2.74, 95% CI: 1.78–4.21), and SWE (OR: 1.05, 95% CI: 1.02–1.08), as shown in Table 3.

Construction of the novel nomogram integrating 2D-SWE values and other independent prognostic factors

The five independent prognostic factors, age, TB, Neu, INR, and SWE identified by multivariate logistic regression analysis, were used to construct a novel nomogram for the prediction of prognosis in the training cohort (Fig. 1). The value of each independent prognostic factor was given a score on a 100-point scale axis, and a total score were calculated by adding up the individual score. The probability to predict the prognosis of patients with ACLF was estimated.

Performance evaluation of the novel nomogram by decision-curve analysis

DCA was conducted to evaluate the clinical utility and net benefit of the new nomogram, which were further compared with those of MELD, MELD-Na, and Jin's model. As shown in Figure 2, the results indicate that the newly developed nomogram had an overall good net benefit within the wide, practical range of threshold probabilities, and impacted patient outcomes.

Performance evaluation and validation of the novel nomogram by ROC curve analysis

The predictive accuracy of the proposed nomogram was evaluated and compared with existing models, including MELD, MELD-Na, and Jin's model. The AUC, sensitivity, and specificity values (Table 4) were calculated using the ROC curves in Figure 3. In the new nomogram, ROCs yielded AUCs of 0.849 in the training cohort and 0.861 in the prospective validation cohort, which were significantly greater than the AUCs of 0.758 for MELD, 0.750 for MELD-Na, and 0.777 for Jin's model in the training cohort (all *p* <0.05, Fig. 3). Table 4 shows that the AUC values for the four models in the test cohort were similar to the values in the training cohort, with the highest AUCs in the newly developed prognosis model. The result along with a high sensitivity and specificity demonstrates the improved discrimination ability of the proposed nomogram to better predict the prognosis of ACLF than MELD, MELD-Na, and Jin's model.

Test of the novel nomogram with the calibration curve analysis

Calibration curves were plotted to assess the agreement between the predicted probability and actually observed probability in the training cohort and test cohorts, which were compared with those of MELD, MELD-Na, and Jin's model. As shown in Figure 4, there was good agreement between prediction by the newly established nomogram and actual observation in the training and test cohorts. The data validate the performance accuracy of the newly developed prognostic nomogram.

Table 1. Demographic characteristics, clinicopathologic features, and laboratory tests of ACLF patients in the training and test cohorts

	Training cohort (n=315)	Test cohort (n=134)	p-value
Sex			0.824
Male (n)	275	118	
Female (n)	40	16	
Age (years)	44	44	0.781
Prognosis			0.084
Nonsurvivor (n)	208	77	
Survivor (n)	107	57	
BMI (kg/m ²)	22.77	22.06	0.411
Liver parenchyma (n)			0.355
Uniform	180	72	
Less uniform	62	23	
Uneven	73	39	
Liver capsule (n)			0.528
Smooth	67	34	
Under smooth	87	35	
Rough	161	65	
Thickness of right liver lobe (mm)	103	102	0.167
Gallbladder wall thickness (mm)	6	6	0.080
Thickening of gallbladder wall (n)			0.832
No	9	19	
Yes	296	125	
Gallbladder enlargement (n)			0.961
No	98	42	
Yes	217	92	
Gallstones (n)			0.294
No	115	42	
Yes	200	92	
Pleural effusion (n)			0.413
No	302	131	
Yes	13	3	
Ascites maximum depth (mm)	40	43	0.589
Portal vein diameter (mm)	12	11	0.419
Umbilical vein re-open (n)			0.546
No	136	62	
Yes	179	72	
Enlarged spleen (n)			0.201
No	98	50	
Yes	217	84	
Splenic portal vein (mm)	7	7	0.617
AST (U/L)	133	137.5	0.719
ALT (U/L)	134	137.5	0.779
ALB (g/L)	33.3	33.2	0.911
TB (μmol/L)	390.8	423.4	0.082

(continued)

Table 1. (continued)

	Training cohort (n=315)	Test cohort (n=134)	p-value
GGT (U/L)	70	69	0.958
ALP (U/L)	135	135.5	0.659
CHE (U/L)	3,681	3,706.5	0.556
Na (mmol/L)	137	137	0.911
Cr (μmol /L)	70.6	72.5	0.556
AFP (ng/ml)	50.6	42.2	0.230
WBC (10 ⁹ /L)	6.55	6.73	0.238
Neu (%)	65.8	67.3	0.512
RBC (10 ⁹ /L)	3.66	3.63	0.959
HGB (g/L)	113	114.5	0.537
PLT (10 ⁹ /L)	98	98.5	0.826
PT (s)	25.1	26.2	0.055
PTA (%)	34	32	0.063
INR	2.28	2.41	0.060
Hepatorenal syndrome	18	8	0.915
Follow-up time (days)	80.0	76.5	0.393
SWE (kPa)	38.5	38.75	0.615

BMI, body mass index; ALT, alanine aminotransferase; AST, aspartate aminotransferase; ALB, albumin; TB, total bilirubin; GGT, γ-glutamyl transpeptidase; CHE, Cholinesterase; ALP, alkaline phosphatase; Na, Sodium; Cr, creatinine; AFP, a-fetoprotein; WBC, white blood cell; Neu, neutrophils; RBC, red blood cell; HGB, hemoglobin; PLT, platelet; PT, prothrombin time; PTA, prothrombin time activity; INR, international normalized ratio; SWE, two-dimensional shear wave elastography.

Table 2. Univariate analysis of prognostic factors in the training cohort

Variable	Odds ratio	95% Confidence Interval (CI)	p-value
Sex			
Male			1
Female	1.19	(0.60–2.37)	0.614
Age*	1.05	(1.03–1.07)	<0.001
BMI	0.94	(0.87–1.01)	0.091
Liver parenchyma			
Uniform			1
Less uniform	1.24	(0.68–2.26)	0.482
Uneven	1.30	(0.73–2.29)	0.375
Liver capsule*			
Smooth			1
Under smooth	2.42	(1.33–4.41)	0.004
Rough	1.87	(0.91–3.83)	0.087
Thickness of right liver lobe*	0.95	(0.93–0.98)	<0.001
Gallbladder wall thickness*	1.10	(1.01–1.18)	0.022
Thickening of gallbladder wall			
No			1
Yes	2.00	(0.65–6.19)	0.228
Gallbladder enlargement			
No			1
Yes	0.98	(0.59–1.62)	0.941

(continued)

Table 2. (continued)

Variable	Odds ratio	95% Confidence Interval (CI)	p-value
Gallstones*			
No			1
Yes	1.66	(1.01–2.74)	0.047
Pleural effusion			
No			1
Yes	1.41	(0.44–4.55)	0.568
Ascites index	1.00	(1.00–1.01)	0.250
Portal vein diameter	1.00	(0.83–1.21)	0.988
Umbilical vein reopen			
No			1
Yes	1.14	(0.71–1.82)	0.598
Enlarged spleen			
No			1
Yes	0.89	(0.54–1.47)	0.660
Splenic portal vein	1.01	(0.86–1.19)	0.873
AST	1.00	(1.00–1.00)	0.985
ALT	1.00	(1.00–1.00)	0.101
ALB*	0.94	(0.89–0.99)	0.011
TB*	1.01	(1.00–1.01)	<0.001
GGT*	1.00	(0.99–1.00)	0.015
ALP	0.99	(0.99–1.00)	0.070
CHE	1.00	(1.00–1.00)	0.554
Na*	0.92	(0.87–0.98)	0.004
Cr*	1.01	(1.00–1.02)	0.017
AFP*	1.00	(1.00–1.00)	0.016
WBC*	1.08	(1.01–1.15)	0.019
Neu*	355.01	(35.34– 3,566.28)	<0.001
RBC	0.92	(0.69–1.21)	0.540
HGB	0.99	(0.98–1.00)	0.066
PLT*	1.00	(0.99–1.00)	0.018
PT*	1.13	(1.09–1.18)	<0.001
PTA*	0.92	(0.89–0.94)	<0.001
INR*	2.82	(2.03–3.91)	<0.001
Follow-up time	0.98	(0.98–0.99)	<0.001
SWE*	1.03	(1.01–1.06)	0.005

**p* < 0.05. BMI, body mass index; ALT, alanine aminotransferase; AST, aspartate aminotransferase; ALB, albumin; TB, total bilirubin; GGT, γ-glutamyl transpeptidase; CHE, Cholinesterase; ALP, alkaline phosphatase; Na, Sodium; Cr, creatinine; AFP, a-fetoprotein; WBC, white blood cell; Neu, neutrophils; RBC, red blood cell; HGB, hemoglobin; PLT, platelet; PT, prothrombin time; PTA, prothrombin time activity; INR, international normalized ratio; SWE, two-dimensional shear wave elastography.

Discussion

To the best of our knowledge, this is the first prospective study to integrate 2D-SWE values with other independent prognostic factors for the prediction of patient prognosis with ACLF-HBV. The novel findings can be summarized as: (1) Univariate and multivariate regression analyses revealed that five independent prognostic factors, including age, Neu,

INR, and 2D-SWE, significantly affect the prognosis of patients with ACLF-HBV. (2) The novel prognostic nomogram was successfully constructed using 2D-SWE values in combination with the other independent prognostic factors to predict the prognosis of ACLF-HBV patients. (3) ROC curve analysis found that the AUCs of the newly constructed model in both the training and the prospective validation cohorts were significantly greater than those of the existing MELD,

Table 3. Multivariate analysis of independent prognostic factors in the training cohort

Variables	Odds Ratio	95% Confidence Interval (CI)	p-value
Age*	1.04	(1.01–1.08)	0.007
BMI	0.93	(0.84–1.04)	0.226
Liver capsule			
Smooth			1
Under smooth	1.84	(0.84–4.05)	0.129
Rough	0.86	(0.32–2.35)	0.776
Thickness of right liver lobe	0.99	(0.95–1.02)	0.465
Thickening of gallbladder wall	1.03	(0.93–1.13)	0.623
TB*	1.01	(1.00–1.01)	<0.001
Na	1.04	(0.96–1.13)	0.294
Neu*	139.55	(6.41– 3,037.71)	0.002
INR*	2.74	(1.78–4.21)	<0.001
SWE*	1.05	(1.02–1.08)	0.003
Gallstones			
No			1
Yes	1.76	(0.91–3.42)	0.094
ALB	0.94	(0.87–1.02)	0.122
GGT	1	(0.99–1.01)	0.848
ALP	1	(0.99–1.01)	0.576
Cr	1	(0.99–1.01)	0.757
AFP	1	(1.00–1.00)	0.326
HGB	1	(0.99–1.02)	0.606
PLT	1	(0.99–1.00)	0.104

*p <0.05. BMI, body mass index; ALB, albumin; TB, total bilirubin; GGT, γ-glutamyl transpeptidase; ALP, alkaline phosphatase; Na, Sodium; Cr, creatinine; HGB, hemoglobin; PLT, platelet; INR, international normalized ratio; SWE, two-dimensional shear wave elastography.

MELD-Na, and Jin’s prognostic models. (4) DCA supported the superior overall net benefit and clinical utility of the newly developed nomogram in predicting the prognosis of ACLF-HBV patients. (5) The novel prognostic nomogram was

well-calibrated according to the good agreement between the predicted and observed probabilities in the calibration curve analysis. The major findings of this study further suggest that the new nomogram has enhanced prognostic ac-

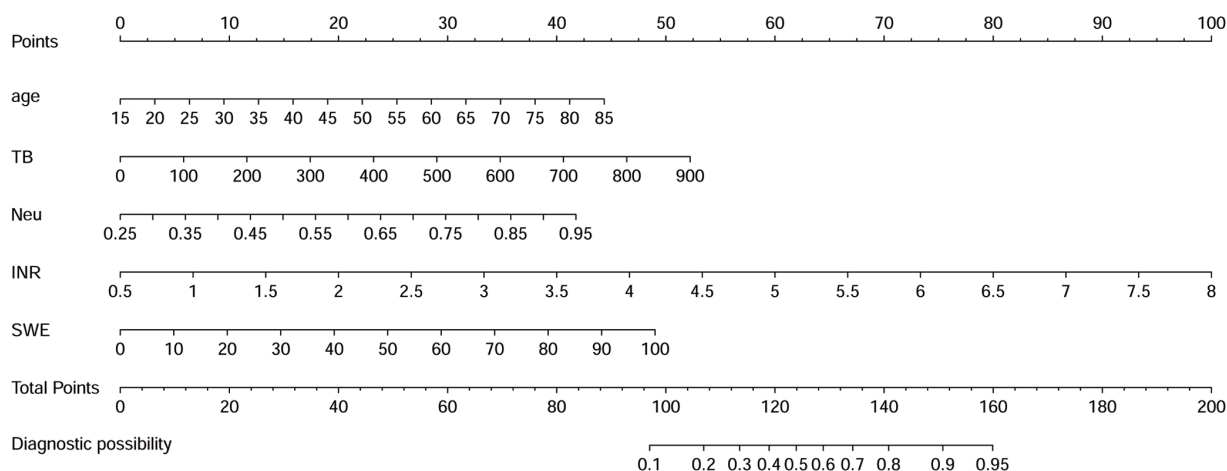


Fig. 1. A novel nomogram for the prediction of the prognosis of patients with ACLF caused by HBV infection. The five factors independently associated with prognosis, age, total bilirubin (TB), neutrophils (Neu), international normalized ratio (INR), and two-dimensional shear wave elastography (2D-SWE) were used to construct the nomogram.

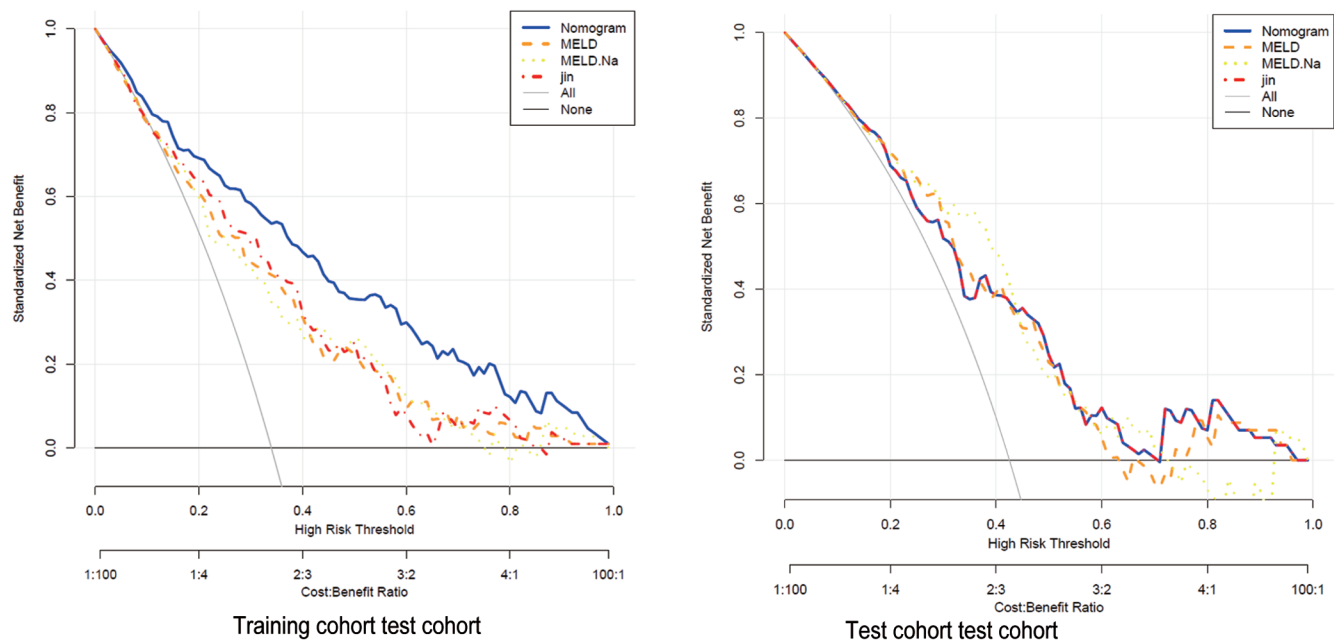


Fig. 2. Decision curves of the newly developed nomogram, MELD, MELD-Na, and Jin's models. Decision curves were plotted to evaluate the clinical utility and net benefit of the new nomogram, which were compared with those of MELD, MELD-Na, and Jin's models. DCA analysis showed that the nomogram had an overall good net benefit within the wide and practical ranges of threshold probabilities and impacted patient outcomes.

curacy, and, therefore appears promising as an improved prognostic tool to be used in the clinical practice.

As in the 2D-SWE-based noninvasive nomogram for predicting the prognosis of ACLF patients, older age, high TB, and INR have been reported to adversely affect the prognosis of ACLF patients in previous studies.^{25,26} Shi et al reported that multivariate time-to-death analysis found older age, high INR, and high levels of serum TB to be independent predictors for early death of ACLF patients, within 28 days.²⁶ In addition, Zheng et al found that a number of variables, including age, TB, serum sodium were significantly correlated with the prognosis of patients with acute-on-chronic hepatitis B liver failure (ACHBLF).²⁵ The previous studies support our findings that these prognostic factors were independently associated with the poor prognosis of ACLF.

Interestingly, this study found that a high percentage of peripheral neutrophils was associated with death or liver transplantation in patients with HBV-related ACLF. Generally, increased neutrophils were believed to be related to bacterial infection, severe systemic inflammation, increased susceptibility to sepsis, or even organ dysfunction. Bacterial infection is an important or even fatal complication of ACLF, and has been related to increased grades of systemic inflammation, worse clinical course, and increased 90-day mortality.²⁷ The underlying mechanisms of the correlations

are not clear, but the interaction of inflammatory mediator and neutrophils in liver failure is a possible explanation. Inflammatory mediators such as IL1, IL8, and TNF α are known promote neutrophil extravasation of liver, trigger neutrophil activation, and in turn kill hepatocytes by inducing oxidative stress and expressing the Fas ligand.²⁸

Recent advances in the use of ultrasound examination for LSM has led the World Health Organization (WHO)⁴ and other professional associations^{10,12} to recommend the use of TE to assess liver fibrosis and cirrhosis, and point out that liver stiffness may be impacted by necrosis or inflammation. Liver necrosis and inflammation may vary with the stage of ACLF-HBV. Studies have found that LSM and MELD had comparable efficacy to predict liver failure,^{11,14-16} and have shown that dynamic monitoring may be beneficial. 2D-SWE is more suitable for obtaining LSM in ACLF than TE because it can be used in patients with ascites. In addition, 2D-SWE is compatible with ultrasound scanners that can evaluate liver morphological changes and potential tumor detection. Previously, Jin's model showed that the MELD-SWE score combined with the MELD and SWE values was better than MELD alone in predicting the prognosis of ACLF-HBV patients.²⁰ In this study, a new model incorporating serological and conventional ultrasound indicators highlights the value of 2D-SWE in predicting the prognosis of chronic and acute

Table 4. Performance comparison of the newly developed model with the existing models

	Training cohort				Test cohort			
	SWE M	MELD	MELD-Na	Jin's	SWE M	MELD	MELD-Na	Jin's
Sensitivity (%)	77.6	67.3	72.0	75.7	66.7	66.7	82.5	75.4
Specificity (%)	77.9	75.0	67.3	70.7	75.3	70.1	32.4	57.1
AUC (95% CI)	0.849 (0.776– 0.779)	0.758 (0.673– 0.750)	0.750 (0.673– 0.720)	0.777 (0.707– 0.757)	0.804 (0.667– 0.818)	0.744 (0.667– 0.727)	0.777 (0.701– 0.825)	0.737 (0.614– 0.792)

AUC, area under the receiver operating characteristic curve.

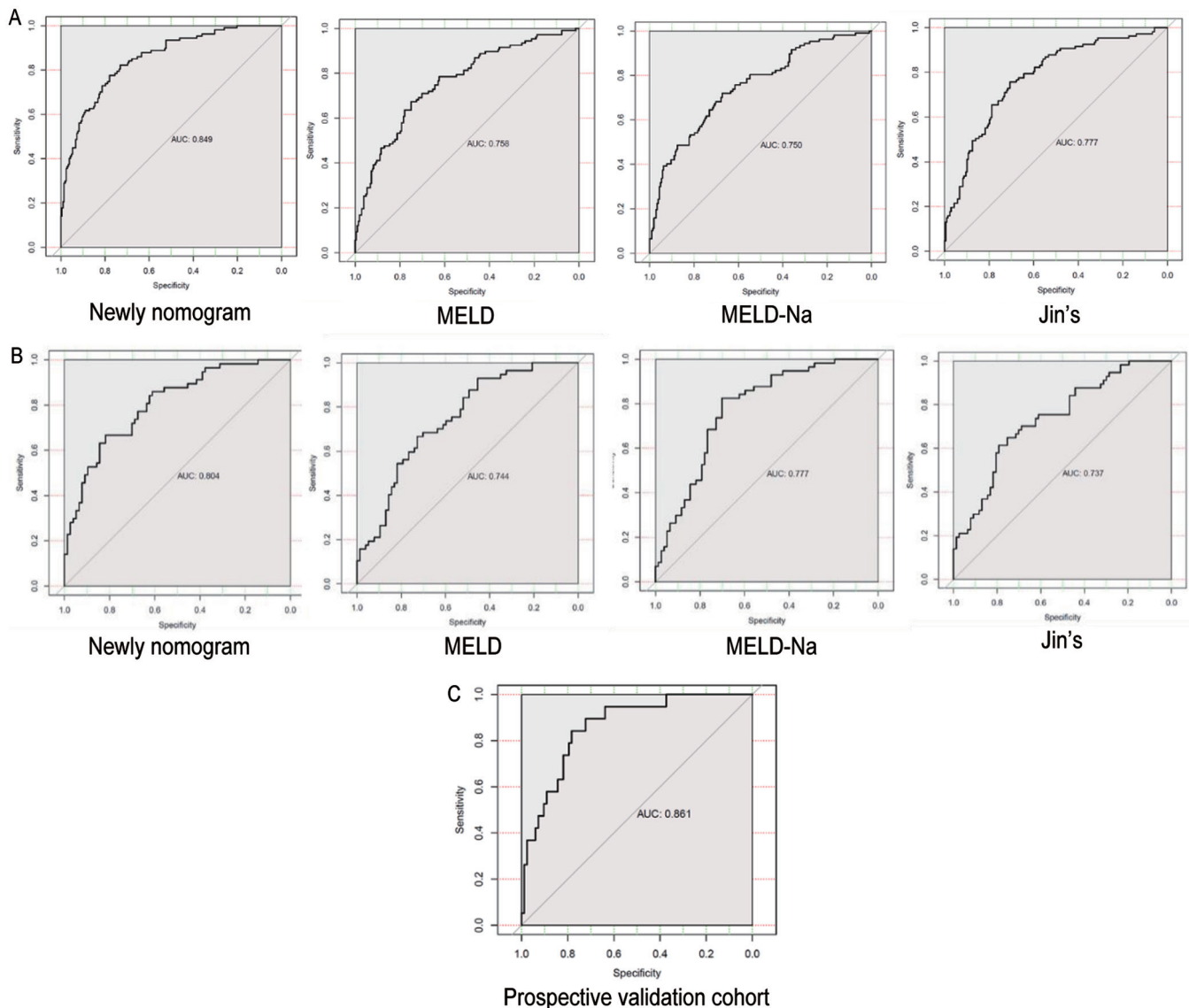


Fig. 3. Receiver operating characteristic (ROC) curves of the newly developed nomogram, MELD, MELD-Na, and Jin's models. ROC curves were plotted to evaluate the accuracy of the newly constructed nomogram, which was compared with the existing models, and validated in the prospective cohort. (A) Training cohort; (B) Test cohort; (C) Prospective validation cohort. The newly developed prognosis model had a greater area under the curve (AUC) than those of MELD, MELD-Na, or Jin's models.

liver failure.

It is pertinent to mention that the constructed nomogram based on 2D-SWE in combination with other four prognostic factors (age, TB, Neu, and INR) was accurate, feasible, and reliable. Its performance was better than that of existing prognostic scoring models, such as MELD, MELD-Na, and Jin's model, for ACLF-HBV patients. First, we conducted the ROC curve analysis to obtain the AUC values. As a result, the AUC value of the newly constructed model was greater than the AUC value of MELD, MELD-Na, and Jin's model. In a previous study, Jalan *et al.*²⁹ reported AUCs of 0.65 for MELD and 0.67 for MELD-Na to predict the 90-day mortality of ACLF patients, and both are lower than the AUC of the newly developed nomogram, which was more accurate than the existing prognostic models in predicting the prognosis of patients with ACLF-HBV. Second, DCA analysis found the overall net benefit and clinical utility of the newly developed nomogram were comparable to the existing prognos-

tic scoring systems or models, i.e., MELD, MELD-Na, and Jin's model, to predict the prognosis of ACLF-HBV patients. Thirdly, the new nomogram was well-validated in the test cohort by calibration curve analysis, indicating good agreement between the predicted and observed probabilities in patients with ACLF-HBV. In addition to our previous findings, the results of this study demonstrate that the new nomogram improved the accuracy of ACLF prognosis and is potentially useful in clinical practice. Considering the relatively high incidence of HBV infection in China, clinical challenges in predicting the prognosis of ACLF caused by HBV infection, and the high mortality of patients with ACLF, this nomogram should be a choice for priority stratification to identify individuals in need of liver transplantation.

Despite the strengths mentioned above, the study has potential limitations. For example, the ACLF-HBV patients in the training, test, and prospective validation cohorts were enrolled from a single hospital in Guangdong province in

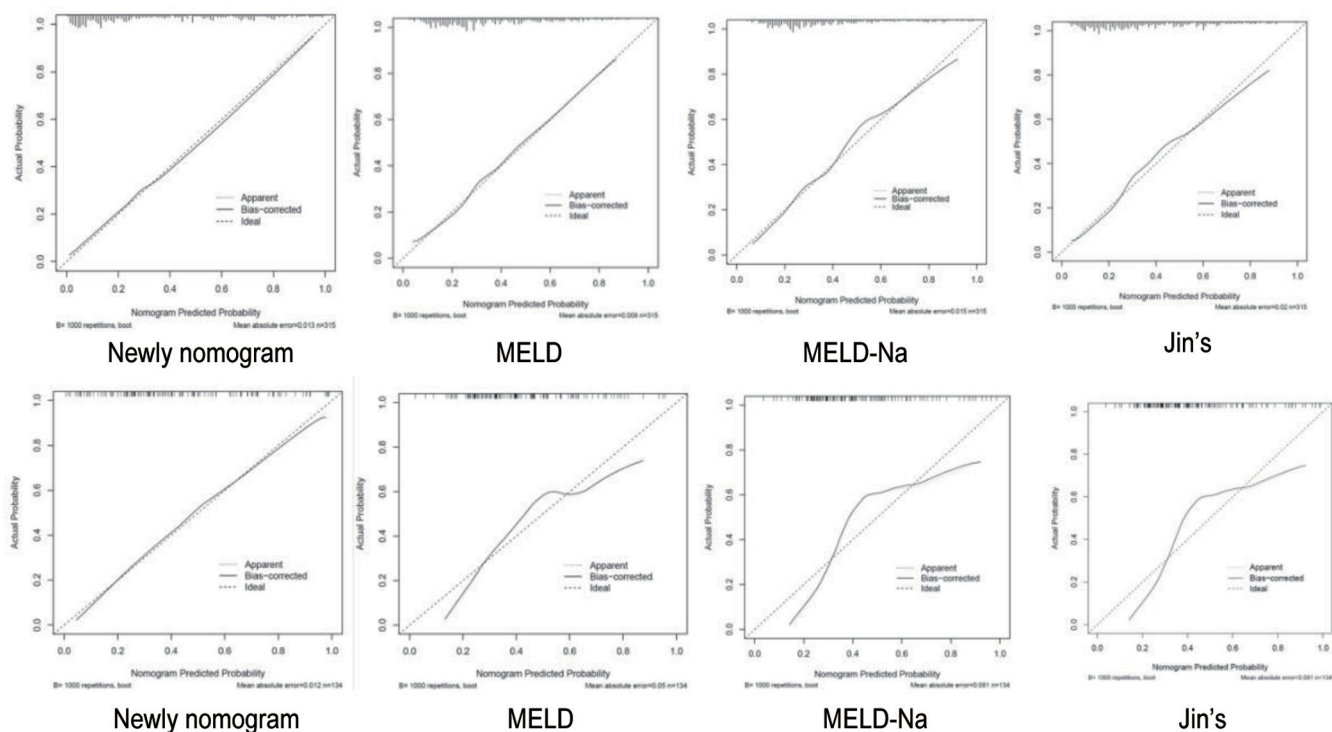


Fig. 4. Calibration curves of the newly developed nomogram, MELD, MELD-Na, and Jin's models. Calibration curves were plotted to assess the agreement between the predicted and actually observed probabilities, which was also compared with the other models. (A) Training cohort; (B) Test cohort. Calibration analysis indicated a good agreement between the prediction by the newly established nomogram and actual observation.

southern China. Future studies should select patients from multiple centers in more diverse geographical areas and among various tiers to yield more representative results. As chronic hepatitis B was identified as the underlying liver disease in these ACLF patients, the newly developed prognostic nomogram may not be applicable to ACLF patients with etiologies other than HBV infection, such as alcohol-related hepatitis, HCV infection, alcohol-related liver diseases, drug-induced hepatitis, autoimmune liver disease, and Wilson's disease, which were excluded from this study. It should be acknowledged that the baseline characteristics were used to develop this model for the early prediction of ACLF prognosis, and that most of the patients did not have multiple organ failures at the time of hospital admission. In this study, we did not compare the model with those taking multiple organ failures into account such as the chronic liver failure-sequential organ failure assessment, or sequential organ failure assessment. It is necessary to externally validate the findings, including the reproducibility, reliability, and accuracy, at multiple centers nationwide.

In conclusion, a novel prognostic nomogram was successfully developed by integrating 2D-SWE values with other independent prognostic factors. The prognostic nomogram had high prognostic accuracy and overall better performance compared with the existing prognostic models. As such, the novel prognostic nomogram may assist hepatologists/surgeons to navigate optimal treatment and management plans, reduce mortality, and ultimately improve the overall care of patients with ACLF-HBV.

Acknowledgments

We thank Jiao Gong (Department of Laboratory Medicine, the Third Affiliated Hospital of Sun Yat-Sen University), for

her assistance with the statistical analysis.

Funding

This study was financially supported by the National Natural Science Foundation of China (81827802) and the National Natural Science Foundation of the Third Affiliated Hospital of Sun Yat-Sen University (2020GZRPYQN17).

Conflict of interest

The authors have no conflict of interests related to this publication.

Author contributions

All authors have made substantial contributions to this study. Conceptual design and writing of the draft manuscript (RZ, JR, LW), acquisition of data (JJ, LW, XhL, XyL, JZ, JW), analysis and interpretation of data (YW, TZ), critical revision of the manuscript (YC, LW, JJ). LW and JJ contributed equally to the work.

Compliance with ethical standards

Each patient provided written informed consent prior to initiating the study. This study was reviewed and approved by the Human Research Ethic Committee of the Third Affiliated Hospital of Sun Yat-Sen University (Guangzhou, Guangdong, China). The study protocol conformed to the ethical

guidelines of the 1975 Declaration of Helsinki.

Data sharing statement

The datasets used and/or analyzed during the current study are available from the corresponding author on reasonable request.

References

- [1] Hernaez R, Sola E, Moreau R, Gines P. Acute-on-chronic liver failure: an update. *Gut* 2017;66(3):541–553. doi:10.1136/gutjnl-2016-312670, PMID:28053053.
- [2] Moreau R, Jalan R, Gines P, Pavesi M, Angeli P, Cordoba J, et al. Acute-on-chronic liver failure is a distinct syndrome that develops in patients with acute decompensation of cirrhosis. *Gastroenterology* 2013;144(7):1426–1437.e9. doi:10.1053/j.gastro.2013.02.042, PMID:23474284.
- [3] Sarin SK, Kedarisetty CK, Abbas Z, Amarapurkar D, Bihari C, Chan AC, et al. Acute-on-chronic liver failure: consensus recommendations of the Asian Pacific Association for the Study of the Liver (APASL) 2014. *Hepatol Int* 2014;8(4):453–471. doi:10.1007/s12072-014-9580-2, PMID:26202751.
- [4] Guidelines for the Prevention, Care and Treatment of Persons with Chronic Hepatitis B Infection. Geneva: World Health Organization. 2015.
- [5] Bernal W, Jalan R, Quaglia A, Simpson K, Wendon J, Burroughs A. Acute-on-chronic liver failure. *Lancet* 2015;386(10003):1576–1587. doi:10.1016/S0140-6736(15)00309-8, PMID:26423181.
- [6] Gustot T, Fernandez J, Garcia E, Morando F, Caraceni P, Alessandria C, et al. Clinical Course of acute-on-chronic liver failure syndrome and effects on prognosis. *Hepatology* 2015;62(1):243–252. doi:10.1002/hep.27849, PMID:25877702.
- [7] Malinchoc M, Kamath PS, Gordon FD, Peine CJ, Rank J, ter Borg PC. A model to predict poor survival in patients undergoing transjugular intrahepatic portosystemic shunts. *Hepatology* 2000;31(4):864–871. doi:10.1053/he.2000.5852, PMID:10733541.
- [8] Sarin SK, Choudhury A, Sharma MK, Maiwall R, Al Mahtab M, Rahman S, et al. Acute-on-chronic liver failure: consensus recommendations of the Asian Pacific association for the study of the liver (APASL): an update. *Hepatol Int* 2019;13(4):353–390. doi:10.1007/s12072-019-09946-3, PMID:31172417.
- [9] Martin P, DiMartini A, Feng S, Brown R Jr, Fallon M. Evaluation for liver transplantation in adults: 2013 practice guideline by the American Association for the Study of Liver Diseases and the American Society of Transplantation. *Hepatology* 2014;59(3):1144–1165. doi:10.1002/hep.26972, PMID:24716201.
- [10] Barr RG, Ferraioli G, Palmeri ML, Goodman ZD, Garcia-Tsao G, Rubin J, et al. Elastography Assessment of Liver Fibrosis: Society of Radiologists in Ultrasound Consensus Conference Statement. *Radiology* 2015;276(3):845–861. doi:10.1148/radiol.2015150619, PMID:26079489.
- [11] Dechene A, Sowa JP, Gieseler RK, Jochum C, Bechmann LP, El Fouly A, et al. Acute liver failure is associated with elevated liver stiffness and hepatic stellate cell activation. *Hepatology* 2010;52(3):1008–1016. doi:10.1002/hep.23754, PMID:20684020.
- [12] Dietrich CF, Bamber J, Berzigotti A, Bota S, Cantisani V, Castera L, et al. EFSUMB Guidelines and Recommendations on the Clinical Use of Liver Ultrasound Elastography, Update 2017 (Long Version). *Ultraschall Med* 2017;38(4):e16–e47. doi:10.1055/s-0043-103952, PMID:28407655.
- [13] Ferraioli G, Filice C, Castera L, Choi BI, Sporea I, Wilson SR, et al. WFUMB guidelines and recommendations for clinical use of ultrasound elastography: Part 3: liver. *Ultrasound Med Biol* 2015;41(5):1161–1179. doi:10.1016/j.ultrasmedbio.2015.03.007, PMID:25800942.
- [14] Karlas TF, Pfrepper C, Rosendahl J, Benckert C, Wittekind C, Jonas S, et al. Acoustic radiation force impulse (ARFI) elastography in acute liver failure: necrosis mimics cirrhosis. *Z Gastroenterol* 2011;49(4):443–448. doi:10.1055/s-0029-1245690, PMID:21476180.
- [15] Kuroda H, Kakisaka K, Oikawa T, Onodera M, Miyamoto Y, Sawara K, et al. Liver stiffness measured by acoustic radiation force impulse elastography reflects the severity of liver damage and prognosis in patients with acute liver failure. *Hepatol Res* 2015;45(5):571–577. doi:10.1111/hepr.12389, PMID:25041122.
- [16] Sharma P, Bansal R, Matin A, Tyagi P, Bansal N, Singla V, et al. Role of Transient Elastography (Fibroscan) in Differentiating Severe Acute Hepatitis and Acute on Chronic Liver Failure. *J Clin Exp Hepatol* 2015;5(4):303–309. doi:10.1016/j.jceh.2015.09.004, PMID:26900271.
- [17] Ferraioli G, Tinelli C, Dal Bello B, Zicchetti M, Filice G, Filice C, et al. Accuracy of real-time shear wave elastography for assessing liver fibrosis in chronic hepatitis C: a pilot study. *Hepatology* 2012;56(6):2125–2133. doi:10.1002/hep.25936, PMID:22767302.
- [18] Ferraioli G, Tinelli C, Zicchetti M, Above E, Poma G, Di Gregorio M, et al. Reproducibility of real-time shear wave elastography in the evaluation of liver elasticity. *Eur J Radiol* 2012;81(11):3102–3106. doi:10.1016/j.ejrad.2012.05.030, PMID:22749107.
- [19] Hudson JM, Milot L, Parry C, Williams R, Burns PN. Inter- and intra-operator reliability and repeatability of shear wave elastography in the liver: a study in healthy volunteers. *Ultrasound Med Biol* 2013;39(6):950–955. doi:10.1016/j.ultrasmedbio.2012.12.011, PMID:23453379.
- [20] Jin JY, Zheng YB, Zheng J, Liu J, Mao YJ, Chen SG, et al. 2D shear wave elastography combined with MELD improved prognostic accuracy in patients with acute-on-chronic hepatitis B liver failure. *Eur Radiol* 2018;28(10):4465–4474. doi:10.1007/s00330-018-5336-z, PMID:29696433.
- [21] Leung VY, Shen J, Wong VW, Abrigo J, Wong GL, Chim AM, et al. Quantitative elastography of liver fibrosis and spleen stiffness in chronic hepatitis B carriers: comparison of shear-wave elastography and transient elastography with liver biopsy correlation. *Radiology* 2013;269(3):910–918. doi:10.1148/radiol.13130128, PMID:23912619.
- [22] Muller M, Gennisson JL, Deffieux T, Tanter M, Fink M. Quantitative viscoelasticity mapping of human liver using supersonic shear imaging: preliminary in vivo feasibility study. *Ultrasound Med Biol* 2009;35(2):219–229. doi:10.1016/j.ultrasmedbio.2008.08.018, PMID:19081665.
- [23] Poynard T, Munteanu M, Luckina E, Perazzo H, Ngo Y, Royer L, et al. Liver fibrosis evaluation using real-time shear wave elastography: applicability and diagnostic performance using methods without a gold standard. *J Hepatol* 2013;58(5):928–935. doi:10.1016/j.jhep.2012.12.021, PMID:23321316.
- [24] Yeh WC, Li PC, Jeng YM, Hsu HC, Kuo PL, Li ML, et al. Elastic modulus measurements of human liver and correlation with pathology. *Ultrasound Med Biol* 2002;28(4):467–474. doi:10.1016/s0301-5629(02)00489-1, PMID:12049960.
- [25] Zheng MH, Shi KQ, Lin XF, Xiao DD, Chen LL, Liu WY, et al. A model to predict 3-month mortality risk of acute-on-chronic hepatitis B liver failure using artificial neural network. *J Viral Hepat* 2013;20(4):248–255. doi:10.1111/j.1365-2893.2012.01647.x, PMID:23490369.
- [26] Shi Y, Zheng MH, Yang Y, Wei W, Yang Q, Hu A, et al. Increased delayed mortality in patients with acute-on-chronic liver failure who have prior decompensation. *J Gastroenterol Hepatol* 2015;30(4):712–718. doi:10.1111/jgh.12787, PMID:25250673.
- [27] Fernandez J, Acevedo J, Wiest R, Gustot T, Amoros A, Deulofeu C, et al. Bacterial and fungal infections in acute-on-chronic liver failure: prevalence, characteristics and impact on prognosis. *Gut* 2018;67(10):1870–1880. doi:10.1136/gutjnl-2017-314240, PMID:28847867.
- [28] Xu R, Huang H, Zhang Z, Wang FS. The role of neutrophils in the development of liver diseases. *Cell Mol Immunol* 2014;11(3):224–231. doi:10.1038/cmi.2014.2, PMID:24633014.
- [29] Jalan R, Saliba F, Pavesi M, Amoros A, Moreau R, Gines P, et al. Development and validation of a prognostic score to predict mortality in patients with acute-on-chronic liver failure. *J Hepatol* 2014;61(5):1038–1047. doi:10.1016/j.jhep.2014.06.012, PMID:24950482.